In situ determination of Earth matter density in a neutrino factory

Hisakazu Minakata* and Shoichi Uchinami†

Department of Physics, Tokyo Metropolitan University, 1-1 Minami-Osawa, Hachioji, Tokyo 192-0397, Japan

(Received 5 December 2006; published 18 April 2007)

We point out that an accurate *in situ* determination of the earth matter density ρ is possible in neutrino factory by placing a detector at the magic baseline, $L = \sqrt{2}\pi/G_F N_e$ where N_e denotes electron number density. The accuracy of matter density determination is excellent in a region of relatively large θ_{13} with fractional uncertainty $\delta\rho/\rho$ of about 0.43%, 1.3%, and $\lesssim 3\%$ at 1σ CL at $\sin^2 2\theta_{13} = 0.1$, 10^{-2}, and 3×10^{-3}, respectively. At smaller θ_{13} the uncertainty depends upon the *CP* phase δ, but it remains small, 3%–7% in more than 3/4 of the entire region of δ at $\sin^2 2\theta_{13} = 10^{-4}$. The results would allow us to solve the problem of obscured *CP* violation due to the uncertainty of earth matter density in a wide range of θ_{13} and δ. It may provide a test for the geophysical model of the earth, or it may serve as a method for a stringent test of the Mikheyev-Smirnov-Wolfenstein theory of neutrino propagation in matter once an accurate geophysical estimation of the matter density is available.

DOI: 10.1103/PhysRevD.75.073013 PACS numbers: 14.60.Pq, 14.60.Lm, 91.50.−r

I. INTRODUCTION

In the past 10 years, the atmospheric [1], the solar [2], and the reactor experiments [3] discovered neutrino oscillation and/or flavor conversion and identified neutrino masses and the lepton flavor mixing as the cause of the phenomena [4–7]. The next goal of the neutrino oscillation experiments is to explore the yet unknown 1–3 sector of the flavor mixing matrix, the Maki-Nakagawa-Sakata matrix [8], namely θ_{13}, the *CP* phase δ, and the neutrino mass hierarchy. If θ_{13} is relatively large, $\sin^2 2\theta_{13} \gtrsim 0.01$, most probably a conventional superbeam [9] can do the job. But, if it turns out to be small, $\sin^2 2\theta_{13} \lesssim 0.01$, it is likely that we need a new technology, either the neutrino factory [10] or the beta beam [11]. Both options are under active consideration [12–14].

In measurement in a neutrino factory, a long baseline distance of several thousand km to a detector is preferred because the event rate increases as muon beam energy gets higher and one wants to keep L/E not too small for oscillation signatures [15]. Then, according to the Mikheyev-Smirnov-Wolfenstein (MSW) theory of neutrino propagation in matter [16,17], the earth matter effect is one of the crucial ingredients in precision measurement of the lepton mixing parameters. It may act as a serious background in determination of *CP* violating phase δ [18–21]. In fact, it has been debated to what extent uncertainty in the earth matter density affects accuracies of determination of lepton mixing parameters, in particular, the *CP* phase δ. See, for example, [22–27].

One way of dealing with the problem of uncertainty of the matter density is to trust geophysical estimation. It appears that there is a consensus in the geophysics community that the uncertainty in the density in the mantle region of the earth is less than 5% [28]. If the uncertainty can be regarded as robust, then the uncertainty may not be so crucial to hurt the accuracy of measurement of the mixing parameters, though it still produces sizable uncertainties. Notice, however, that the authors of [24] take a much more conservative attitude in estimating the uncertainty of the matter density. See e.g., [27] for a recent estimation of impact of the matter density uncertainty on accuracy in mixing parameter determination.

However, it would be much nicer if neutrino factory experiments can measure *in situ* the average matter density in the mantle region of the earth. It is not completely satisfactory that the most advanced apparatus for precision measurement of the lepton mixing parameters has to rely on the parameter that cannot be directly measured. In fact, the same attitude is shared by the authors of the pioneering work of neutrino factory analysis [15], in which the accuracy of matter density determination by a neutrino factory is estimated. Describing an improved way for the *in situ* measurement of the earth matter density in a neutrino factory is nothing but the goal of this paper. The recent progress in understanding of how to lower the analysis energy threshold [29] will be the key to the remarkable accuracy we will uncover.

Moreover, measured matter density in the deep interior of the earth by neutrinos would offer an independent test for the theory of earth structure and its formation. Note that the mantle region contains 70% of the earth mass. If it is significantly different from the value predicted by geophysical models (after taking account of the uncertainties in both prediction and measurement), we have to think about at least one of the following possibilities: (1) A drastic revision of the geophysical model of the earth must be attempted. (2) The MSW theory of neutrino propagation is in error. We hope that this discussion is illuminative of the importance of the neutrino measurement of the earth matter density.

The chondrite earth model with constraint of seismic data results in an earth model with several layers and the

*Electronic address: minakata@phys.metro-u.ac.jp
†Electronic address: uchinami@phys.metro-u.ac.jp

matter density in each layer can be predicted with reasonable precision with the constraint of accurately measured earth mass. In particular, the density in the mantle region seems to be obtained with the least uncertainties [30]. If the geophysical estimation can be regarded as robust the neutrino factory measurement of matter density we propose in this paper severely tests the theory of neutrino propagation in matter. Notice that the matter density at the solar core is currently measured by using neutrinos only up to a factor of ~ 2 uncertainty [31]. Neutrino tomography of the earth by using accelerator and other neutrino sources has been discussed in many literatures [32–35].

In Sec. II, we give three conditions for accurate measurement of the earth matter density based on general considerations. In Sec. III, we discuss what is the baseline that is most sensitive to matter density change. In Sec. IV, we describe a concrete way of determining the earth matter density by neutrino factory. In Sec. V, we define the statistical method for analysis. In Sec. VI, we describe the results of our analysis. In Sec. VII, we address the problem of δ-dependence of the error of matter density determination. In Sec. VIII, an iterative procedure for combined analysis of data at the intermediate and the far detectors is described. In Sec. IX, we give concluding remarks.

II. GENERAL CONSIDERATIONS

Experiments which aim at measuring the earth matter density accurately by using neutrino oscillation must satisfy a few crucial requirements. First, the matter effect must be sizable, at least comparable with the vacuum oscillation effect. The relative importance between the vacuum and the matter effects in long-baseline (LBL) neutrino oscillation experiments may be quantified by comparing the following two dimensionless quantities:

$$\Delta_{31} \equiv \frac{|\Delta m^2_{31}|L}{4E} = 1.27\left(\frac{|\Delta m^2_{31}|}{10^{-3}\ \mathrm{eV}^2}\right)\left(\frac{L}{1000\ \mathrm{km}}\right)\left(\frac{E}{1\ \mathrm{GeV}}\right)^{-1} \quad (1)$$

$$aL \equiv \frac{1}{\sqrt{2}} G_F N_e L = 0.27\left(\frac{\rho}{2.8\ \mathrm{g/cm}^3}\right)\left(\frac{L}{1000\ \mathrm{km}}\right), \quad (2)$$

where a is related to neutrino's index of refraction with G_F being the Fermi constant and N_e the electron number density in the earth. N_e is related to the matter density ρ as $N_e = Y_e N_A \rho$ with Avogadro's number N_A and the electron fraction Y_e. We take $Y_e = 0.5$. In most cases, the experimental setup is such that $\Delta_{31} \sim \pi/2$ to maximize the appearance signal. In view of (2), the matter effect plays no significant role in settings of baseline less than ~ 1000 km.

A sizable matter effect is certainly a necessary but *not* a sufficient condition for experiments to measure the matter density. What is important is the sensitivity to artificial matter density change $\delta\rho$. To quantify the sensitivity one has to have a variable experimental parameter through which one can control relative importance of the matter effect to that of the vacuum oscillation. Since aL/Δ_{31} is proportional to E the natural candidate for relevant experimental parameters to vary would be the neutrino energy.

It is not the end of the list of requirements. A measurement at a given setup determines a combination of the mixing parameters, typically θ_{13}, δ, and the matter effect coefficient a. Unless the former two parameters are separately measured in experiments in vacuum,[1] the coefficient a or the matter density alone cannot be cleanly determined by any single measurement. Generally speaking, the condition is hard to be met because most of the projects to determine unknowns in the lepton flavor mixing are designed to be sensitive not only to the CP phase δ, but also to the matter effect, which is required to determine the mass hierarchy.

In summary, we list here the three requirements (A)–(C); (A) sensitivity to the matter effect. (B) existence of $\delta\rho$ sensitive tunable parameters. (C) mixing parameter independent measurement of the matter density. We will discuss in the following sections below how these requirements can be satisfied.

III. WHICH BASELINE? PRELIMINARY CONSIDERATION WITH ENERGY SCAN

In this paper, we focus on neutrino factory measurement of the earth matter density. Since the largest part of the straight line path of neutrinos is in the mantle region of the earth in the neutrino factory, what we mean by the matter density in this paper is that of the mantle region. Precisely speaking, the matter density we try to determine is an averaged value along the neutrino trajectory.

The first question we must address is: What is the appropriate baseline distance for the measurement? We try to find an answer to this question by choosing muon beam energy as the tunable parameter, the energy scan. Namely, we consider the neutrino factory measurement of numbers of appearance events $\nu_e \to \nu_\mu$ at two different muon beam energies. It will give us the normalized event number difference $\Delta N/N$. The question we address here is what is the baseline L that gives rise to the strongest response in $\Delta N/N$ to matter density change.

For simplicity, we employ in this section the asymptotic expansion of the oscillation probability assuming $\Delta_{31} \ll 1$.[2] The standard formula for $\nu_e \to \nu_\mu$ appearance

[1] MEMPHYS [36] would be an ideal apparatus for this purpose because even the T2K experiment [37] is contaminated by the matter effect which leads to some sensitivities to the mass hierarchy in a limited region of δ, as anticipated [21,38] and proved by the recent analyses [39].

[2] In a standard setting, Δ_{31} is small; $\Delta_{31} = 0.24\left(\frac{\Delta m^2}{2.5\times 10^{-3}\ \mathrm{eV}^2}\right) \times \left(\frac{L}{3000\ \mathrm{km}}\right)\left(\frac{E}{40\ \mathrm{GeV}}\right)^{-1}$.

probability [15] [for its full expression, see (12) in Sec. VII] takes the form at high energies, $\Delta_{31} \equiv (\frac{\Delta m^2_{31} L}{4E}) \ll 1$, as

$$P(\nu_e \to \nu_\mu) = \frac{A}{E^2} + \frac{B}{E^3} \tag{3}$$

where E is the neutrino energy and L is the baseline distance. The coefficients A and B are given to leading order in s_{13} by

$$\begin{aligned} A &= \left(\frac{\sin aL}{aL}\right)^2 \left(\frac{|\Delta m^2_{31}|L}{4}\right)^2 [4 s^2_{23} s^2_{13} \\ &\quad \pm 4 \sin 2\theta_{12} c_{23} s_{23} \epsilon s_{13} \cos\delta + c^2_{23} \sin^2 2\theta_{12} \epsilon^2] \\ B &= \pm 4 \left(\frac{\sin aL}{aL}\right)^2 \left(\frac{|\Delta m^2_{31}|L}{4}\right)^3 g(aL) \\ &\quad \times \left[2 s^2_{23} s^2_{13} + \sin 2\theta_{12} c_{23} s_{23} \epsilon s_{13} \cos\delta \left(1 \pm \frac{\tan\delta}{g(aL)}\right)\right], \end{aligned} \tag{4}$$

where $\epsilon \equiv |\frac{\Delta m^2_{21}}{\Delta m^2_{31}}|$, and $a = G_F N_e/\sqrt{2}$ as before. The function g is defined by $g(x) = 1/x - \cot x$. The positive and the negative sign in (4) are for the normal and the inverted mass hierarchies, respectively. In (4) and throughout this paper, we use the constant matter density approximation.

It is well known that the integrated electron neutrino flux $F_{\nu e}$ from muon decay has energy distribution as $F_{\nu e}(E) = F_0 y^2(1-y)$ (in units of number of ν's per unit area) where $y \equiv \frac{E}{E_\mu}$ and $F_0 = \frac{12}{\pi} \frac{n_\mu E_\mu}{L^2 m^2_\mu}$ with n_μ and L being the number of useful muon decay and the baseline distance, respectively. Then, the number of wrong sign muon events is given, using the number of target atom N_T, and by approximating the energy dependence of the charged current (CC) cross section as linear, $\sigma_{\rm CC} = \sigma_0 E$, as

$$\begin{aligned} N(E_\mu) &= N_T \int_{E_{\rm th}}^{E_\mu} dE F_e(E) \sigma_{\rm CC}(E) P(\nu_e \to \nu_\mu; E) \\ &= \frac{2}{\pi} \frac{n_\mu}{L^2 m^2_\mu} \sigma_0 N_T (E_\mu A + 3B) \end{aligned} \tag{5}$$

where we have assumed that the muon's threshold energy $E_{\rm th}$ can be made low enough to allow the approximation $1 \gg \frac{E_{\rm th}}{E_\mu} \simeq 0$.

Let us consider measurement at two adjacent muon beam energies E_μ and $E_\mu + \Delta E_\mu$ with number of events $N(E_\mu)$ and $N(E_\mu + \Delta E_\mu)$, and define their difference as $\Delta N \equiv N(E_\mu + \Delta E_\mu) - N(E_\mu) \simeq \frac{dN(E_\mu)}{dE_\mu} \Delta E_\mu$. We define the double ratio $\frac{\Delta N}{N} / \frac{\Delta E_\mu}{E_\mu}$, which is independent of the uncertainties in the CC cross section, the neutrino flex, the baseline, and the number of target atoms. We obtain

$$\frac{\frac{\Delta N}{N}}{\frac{\Delta E_\mu}{E_\mu}} = \frac{1}{1 + 3\frac{B}{E_\mu A}}. \tag{6}$$

Now, the crucial question we have to ask is: What is the baseline distance for which variation of the matter density, or a, induces maximal changes in the double ratio? From (6), it is the place where B/A changes significantly when aL is varied. The answer is $aL = \pi$ at which $g(aL)$ (which is proportional to B/A) diverges. This distance is nothing but the one called the "magic baseline" in the literature [40]. It is interesting to see that the magic baseline appears in our treatment as a point where the sensitivity to matter density variation is maximal. The length has been known in the theory of neutrino propagation in matter as "refraction length" [16]. For a recent discussion on the meaning of the magic baseline, see [41].

Despite the fact that the asymptotic expansion is not valid at around the distance where $g(aL)$ diverges, one can show, by using the full expression of the oscillation probability, that the distance comparable to the magic baseline is indeed the most sensitive place for the double ratio to change in matter density. (See Fig. 5.1 of [42].) Thus, the asymptotic expansion is a correct indicator for the right baseline distance for measurement of the matter density. (It is reminiscent of the feature that the one-loop QCD coupling constant diverges at the hadronic scale Λ.)

IV. MEASURING EARTH MATTER DENSITY AT THE MAGIC BASELINE; ENERGY BINNING

We now switch to a different strategy of using neutrino energy as the tunable parameter, though we will make a brief comment on the method of energy scan at the end of Sec. VI. We consider measurement of the earth matter density at the magic baseline

$$L = \frac{\sqrt{2}\pi}{G_F N_e} = 7480 \left(\frac{\rho}{4.2\ {\rm g/cm^3}}\right)^{-1} {\rm km}. \tag{7}$$

As was emphasized in the original article [40], one of the most characteristic features of the magic baseline is that the oscillation probability $P(\nu_e \to \nu_\mu)$ is independent of the CP violating phase δ [43]. Then, one can measure θ_{13} independently of δ, and this property has been utilized to resolve the parameter degeneracy by combining with the detector at $L = 3000$–4000 km in the neutrino factory measurement of θ_{13} and δ [27,40]. We will show below that the property is also the key to our method for accurate measurement of the earth matter density, fulfilling the requirement (C) at least partly. We, however, encounter below the problem of unexpected δ-dependence in a limited region of θ_{13} and δ. See Sec. VII.

Now, the key question is: What is the most efficient way to measure the matter density accurately at the magic baseline? To formulate the right strategy for this purpose we analyze the structure of the appearance probability $P(\nu_e \to \nu_\mu)$. At around the magic baseline the Cervera *et al.* formula [15] has a very simple form with vanishingly small solar and interference terms [the first term in (12) in

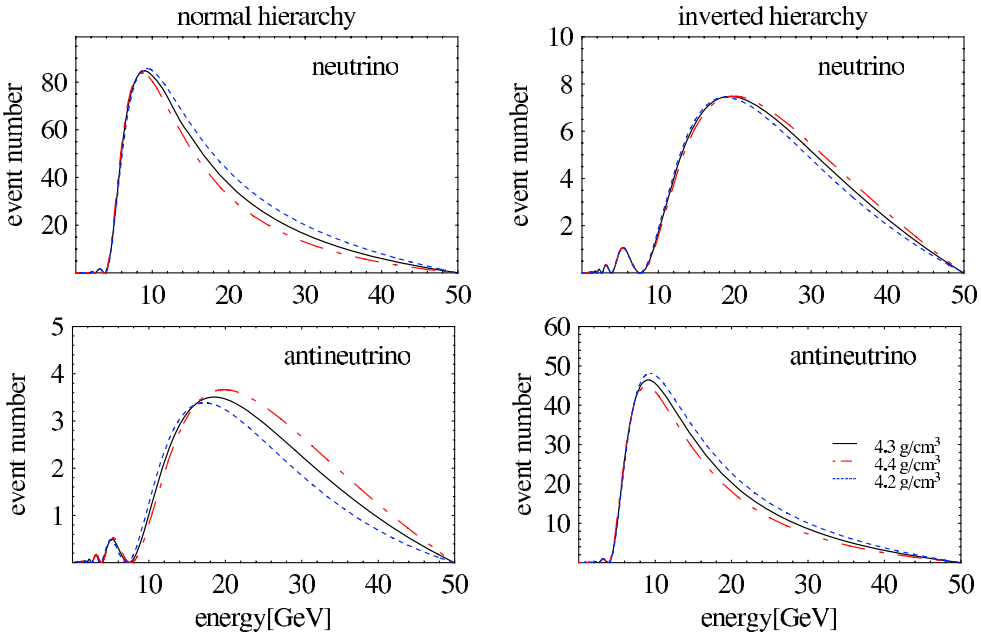

FIG. 1 (color online). The energy distribution of event number (per GeV) is plotted with three values of the matter density, 4.2 g/cm^3 (shown in blue dotted curve), 4.3 g/cm^3 (black solid), and 4.4 g/cm^3 (red dash-dotted). The left and the right two panels in Fig. 1 are for the cases of the normal and the inverted mass hierarchies, respectively. The mixing parameters are taken as $\delta = 0$ and $\sin^2 2\theta_{13} = 0.01$.

Sec. VII],

$$P(\nu_e \to \nu_\mu) = s_{23}^2 \sin^2 2\theta_{13} \left[\frac{\Delta_{31} \sin(aL \mp \Delta_{31})}{(aL \mp \Delta_{31})} \right]^2 \quad (8)$$

with $aL = \pi$, where the $\pm$ sign in (8) corresponds to the neutrino and the antineutrino channels. We note that when the matter density is perturbed, $\rho \to \rho + \delta\rho$, or $aL = \pi + \epsilon$ at the magic baseline, the response of the function in the square bracket in (8) is given as follows:

$$\frac{\sin(aL \mp \Delta_{31})}{(aL \mp \Delta_{31})} = \frac{\sin(\pi \mp \Delta_{31})}{(\pi \mp \Delta_{31})} [1 - \epsilon g(\pi \mp \Delta_{31})] \quad (9)$$

where $g(x) \equiv 1/x - \cot x$ as before.[3] Equation (9) indicates that the response to density change depends upon the neutrino energy, the channel (ν or $\bar{\nu}$), and the neutrino mass ordering, the normal ($\Delta_{31} > 0$), or the inverted ($\Delta_{31} < 0$) hierarchies.

For definiteness, we first discuss the case of the normal hierarchy ($\Delta_{31} > 0$). In the neutrino channel, the equation $g(\pi - \Delta_{31}) = 0$ has a solution at $\Delta_{31} - \pi = 0$. Namely, the critical energy is given by $E_c \simeq 7.6$ GeV for $L = 7500$ km. Since $g(x)$ is an odd function of x, the probability decreases (increases) at neutrino energies $E > E_c$ ($E < E_c$) as the density increases in the neutrino channel. In the antineutrino channel, the equation $g(\pi + \Delta_{31}) = 0$ has a solution at $\Delta_{31} + \pi = 4.493$, and $g(x) > 0$ for $x > 4.493$ and vice versa. The corresponding critical energy is $E_c \simeq 17.6$ GeV. The antineutrino probability increases (decreases) at neutrino energies $E > E_c$ ($E < E_c$) as the density increases, a behavior opposite to the neutrino channel. In the inverted hierarchy, the situation of the neutrino and the antineutrino channels completely reverses, as one can easily confirm.

In Fig. 1, the event number distributions are plotted as a function of neutrino energy with three values of the matter densities. 4.2, 4.3, and 4.4 g/cm^3. The mixing parameters are taken as $\delta = 0$ and $\sin^2 2\theta_{13} = 0.01$. The left and the right two panels of Fig. 1 are for the cases of the normal and the inverted mass hierarchies, respectively. Notice that the oscillation probability is the only piece that is sensitive to matter density variation, and hence our above estimation of the critical energy should apply to the event number distribution as well. Figure 1 confirms the qualitative behavior expected by the above analysis of response of the oscillation probability to the matter density perturbation. The difference between the critical energies in the neutrino and the antineutrino channel, as well as the characteristic feature is obvious: Smaller (larger) number of events in the neutrino (antineutrino) channel at energies above E_c for higher matter density in the normal hierarchy case (and a completely reversed feature in the inverted hierarchy case).

[3]It may be instructive to remark that $g(x)$ is a monotonically increasing function of x in a range $2n\pi < x < (2n+1)\pi$ where n is an integer. It has zero at $x = 0$ and at $x = 4.493$, and diverges to $\pm\infty$ at $x = n\pi \mp \epsilon$.

Therefore, it appears that one can expect the largest sensitivity to the matter density by using the two energy bins below and above E_c. The opposite response of the neutrino and the antineutrino channels to the matter density variation suggests that higher sensitivity can be achieved by using both channels, which will be verified in Sec. VI.

We emphasize that lowering the analysis threshold, the possibility under active investigation [29], is the key to the feasibility of our method of energy binning, because the information below $E \lesssim 10$ GeV is quite essential for neutrino (antineutrino) channel for the normal (inverted) hierarchy. We used the formula (5) but with the exact expression of the oscillation probability [44] to compute the number of events with suitable modification of the range of integration over neutrino energy. In our analysis in this paper we use only the signal events by the charged current (CC) reaction. We take the cross section of CC reactions (including deep inelastic reactions) $\sigma_{\rm CC} = 0.67 \times 10^{-38} (E/{\rm GeV})\ {\rm cm}^2$ for neutrinos and $\sigma_{\rm CC} = 0.34 \times 10^{-38} (E/{\rm GeV})\ {\rm cm}^2$ for antineutrinos [15] in our analysis. Throughout this paper, apart from the comment at the end of Sec. VI A, the true values of the neutrino mixing parameters are assumed as follows: $|\Delta m^2_{31}| = 2.5 \times 10^{-3}\ {\rm eV}^2$, $\Delta m^2_{21} = 7.9 \times 10^{-5}\ {\rm eV}^2$, $\sin^2 2\theta_{12} = 0.86$, and $\sin^2 2\theta_{23} = 1$.

In principle the disappearance channel $\nu_\mu \to \nu_\mu$ can be added to the analysis within the setting of a magnetized iron detector. We do not go into this task in this paper. Though the matter effect is known to be sizable at these distances [45], the response to matter density change does not appear to be favorable.

V. ANALYSIS METHOD

A. Experimental setting

In this paper, we consider a setting of neutrino factory with muon energy $E_\mu = 50$ GeV and assume total 3×10^{21} useful muon decays per each polarity, as quoted in [46]. It may require 5–10 years of operation of the muon storage ring depending upon its luminosity.[4] Our basic attitude is that operation of the neutrino factory will be coordinated by the requirement of optimization for accurate measurement of *CP* phase δ and θ_{13}. Therefore, measurement of the matter density should be carried out as a ''by-product'' within a given schedule optimized for the above purpose.

A standard setting of the neutrino factory includes two magnetized iron detectors, one at baseline $L =$ 3000–4000 km and the other at the magic baseline $L =$ 7500 km, which will be denoted as the intermediate and the far detectors, respectively. Note that the distance to the far detector does not exactly coincide with the magic baseline as given in (7) if the matter density is 4.3 g/cm^3, for example. But, the discrepancy of this level should be admitted because it is unlikely that we can find a site for the far detector at the distance equal to the magic baseline in a mathematical precision. Note also that for $L =$ 7500 km neutrino passes through the lower mantle region in more than half a fraction of its trajectory and its maximum depth is about 1220 km.

In this paper, we analyze only the data taken by the far detector, leaving a full analysis of the data at the intermediate and the far detectors for future work. As a way of effectively implementing the information obtained by the intermediate detector, we impose the constraint on δ in doing fit in the analysis of far detector data. The fiducial mass of the far detector is assumed to be 40 kton. We also assume that the efficiency of event reconstruction is 80% and is independent of energy, which appears to be a good approximation to the efficiency in most of the relevant energy region shown in [29].[5] See also [48] for the plot.

We now argue that analyzing only the data of the far detector is a sensible first approximation. To a good approximation there is a separation between the intermediate and the far detectors about their functions. The far detector has little sensitivity to the *CP* violating phase δ, and the sensitivity to it solely comes from the intermediate detector. The matter effect, which is crucial in determining the earth matter density, is mainly felt by the far detector. Though θ_{13} is determined jointly by the intermediate and the far detectors, the latter is crucial to resolve degeneracy to precisely measure θ_{13} and δ [40]. In fact, we will show that the maximally achievable accuracy of determination of the matter density only with the far detector is already quite remarkable, $\simeq 1\%$ ($\simeq 2\%$) level for $\sin^2 2\theta_{13} = 0.01$ (0.001) at 1σ CL, as will be shown in Sec. VI.

B. Statistical procedure for quantitative analysis

In our analysis, we use two energy bins, 5 GeV $\le E \le$ 10 GeV and 10 GeV $\le E \le$ 50 GeV for neutrino, and 5 GeV $\le E \le$ 20 GeV and 20 GeV $\le E \le$ 50 GeV for antineutrino channels for the reasons discussed in Sec. IV. Notice that the boundary between the low- and the high-energy bins is somewhat different between the neutrino and the antineutrino channels, as can be seen as appropriate in Fig. 1. While we do not explicitly deal with the issue of finite resolution in the reconstructed neutrino energy it will be partially taken care of by the systematic error discussed below.

[4]The authors of [25,27] assume a more modest value of total 2×10^{21} useful muon decays per each polarity. On the other hand, if the ''reference neutrino factory'' setting [47] is realized one may be able to accumulate 5×10^{21} muon decays by 5 years of operation per polarity.

[5]The efficiency presented in these references is a preliminary one and is undergoin further improvement. The currently estimated efficiency may be lower than 80% at energies at around 5 GeV. However, our optimistic assumption may not hurt the sensitivity estimate significantly because the event numbers which come from this region are rather small.

The definition of $\Delta\chi^2$ for our analysis is given by

$$\Delta\chi^2 \equiv \min_{\alpha's} \sum_{a=\nu,\bar{\nu}} \left[\sum_{i=1}^{2} \left\{ \frac{(N_{ai}^{\rm obs} - (1+\alpha_i+\alpha_a+\alpha)N_{ai}^{\rm exp})^2}{N_{ai}^{\rm exp} + \sigma_{pb}^2 (N_{ai}^{\rm exp})^2} + \frac{\alpha_i^2}{\sigma_{Pb}^2} \right\} + \frac{\alpha_a^2}{\sigma_{pB}^2} \right] + \frac{\alpha^2}{\sigma_{PB}^2}, \tag{10}$$

where $N_{ai}^{\rm obs}$ is the number of events in ith bin computed with the values of input parameters, and $N_{ai}^{\rm exp}$ is the one computed with a certain trial set of parameters. The form of $\Delta\chi^2$ with the notation of errors is analogous to that used in [49]. The generalization to measurement at multiple energy bins, if necessary, is straightforward.

The nature of the errors σ_{PB}, σ_{Pb}, σ_{pB}, and σ_{pb} and the examples of them are as follows. For simplicity of notation, we call the following errors as the category A; detection efficiency, energy resolution, and efficiency in muon charge identification. We assume that the dominant part of the category A errors are correlated between ν and $\bar{\nu}$ channels. This assumption can be relaxed, if necessary.

(i) σ_{PB} ($\nu - \bar{\nu}$ and bin-by-bin correlated error): Uncertainties in detector volume, energy-independent component of the category A errors.

(ii) σ_{Pb} ($\nu - \bar{\nu}$ correlated but bin-by-bin uncorrelated error): Energy-dependent component of the category A errors.

(iii) σ_{pB} ($\nu - \bar{\nu}$ uncorrelated but bin-by-bin correlated error): Uncertainties in beam energy estimate, neutrino flux estimate, energy-independent part of reaction cross section error.

(iv) σ_{pb} (uncorrelated error): Energy- and channel-dependent fluctuation of the category A errors, etc., which should be very small.

We take, without any solid information for these errors at this moment, $\sigma_{PB} = \sigma_{Pb} = \sigma_{pB} = 2\%$ and $\sigma_{pb} = 1\%$ in our analysis. The expected small values of the errors are partly based on the fact that the uncertainties in the muon energy and the luminosity are negligibly small for our present purpose [12,50]. We also examine the stability of the results by relaxing these errors by a factor of 2. We will see that measurement is still dominated by the statistical error and a much smaller uncorrelated error, $\sigma_{pb} = 0.1\%$, would lead to a minor improvement.

C. Treatment of CP phase δ

Despite the fact that δ-dependence is expected to be absent at the magic baseline, the proper procedure of the analysis has to include varying over δ during the fit. The best way to do this is to carry out a combined analysis of data taken by both the intermediate and the far detectors. Leaving it to a future work, we give in this paper a simplified treatment by mimicking data at the intermediate detector by a constraint imposed on δ by adding the term

$$\Delta\chi_\delta^2 = \left(\frac{\delta - \delta_{\rm input}}{\sigma_\delta} \right)^2 \tag{11}$$

in $\Delta\chi^2$ in (10). We have chosen $\sigma_\delta = 0.35$ (20°) as a representative value based on the estimation of the width of the χ^2 parabola at around the local minimum as given in [51].

We note that "by definition" of the magic baseline, the procedure of varying over δ should give no significant effect. In fact, we have confirmed that the property holds in a wide region of θ_{13} and δ, apart from the one with a subtle feature to be addressed in Sec. VII. We have also confirmed that using a factor of 2 larger value of σ_δ does not produce visible changes in the results in the entire region.

VI. ANALYSIS RESULTS

A. Analysis with fixed δ

We first discuss the results with fixed δ to have better understanding of the structure of analysis of the far detector and the roles of the systematic errors without worrying about influence of δ.

In Fig. 2, presented is the region in $\sin^2 2\theta_{13} - \rho$ space allowed by measurement of ν_μ and $\bar{\nu}_\mu$ appearance events with our reference setting of neutrino factory. The confidence level (CL) contours are defined with 2 degrees of freedom (DOF) in Fig. 2. The input matter density is taken as $\rho = 4.3$ g/cm^3. The normal mass hierarchy is assumed and δ is taken to be zero. The true values of $\sin^2 2\theta_{13}$ is assumed to be 0.01 and 0.001 in the left and right two panels, respectively. The upper and the lower two panels are for the systematic errors given in Sec. V B and the twice larger values than those, respectively. Notice that the region is compact not only in ρ direction but also in $\sin^2 2\theta_{13}$ direction despite the fact that we have analyzed the data at the far detector only. [If the binning of the data were not done the analysis would yield a prolonged contour in $\sin^2 2\theta_{13} - \rho$ space, as one expects from (8).] It is due to a high sensitivity to θ_{13} at the magic baseline which stems from that the probability is free from δ. It is impressive to see this behavior because the statistics is quite small due to the long baseline, as can be seen in Fig. 1.

As indicated in the lower two panels in Fig. 2, a factor of 2 enlarged systematic errors gives a relatively minor effect on $\delta\rho/\rho$, making the original uncertainty 1.3% (2.8%) to a modestly larger value 1.4% ($^{+2.9}_{-2.8}$%) both at 1σ CL at $\sin^2 2\theta_{13} = 0.01$ (0.001). On the other hand, the enlarged systematic errors gives a larger effect on θ_{13}, worsening the original uncertainty of $\sin^2 2\theta_{13}$ from ($^{+8}_{-6}$%) to ($^{+12}_{-10}$%) [($^{+19}_{-15}$%) to ($^{+21}_{-16}$%)] at 1σ CL at $\sin^2 2\theta_{13} = 0.01$ [0.001]. The fact that a factor of 2 relaxed systematic errors lead to only modest increase of $\delta\rho/\rho$ must be emphasized. The tendency is more prominent for $\sin^2 2\theta_{13} = 0.001$. It is because the detector at the magic baseline is highly sensi-

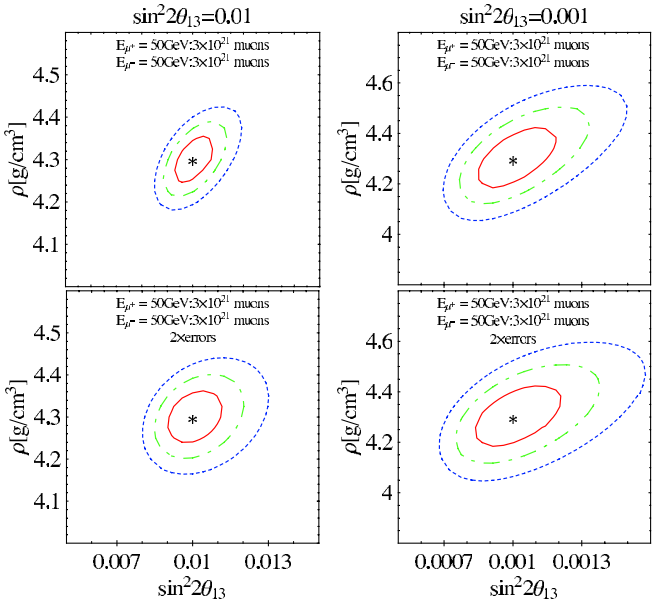

FIG. 2 (color online). Regions in $\sin^2 2\theta_{13} - \rho$ space allowed by operation of the neutrino factory with 3×10^{21} useful muon decays per each polarity watched by 40 kton magnetized iron detector at $L = 7500$ km. The red solid, the green dash-dotted, and the blue dotted lines are for contours at 1, 2, and 3σ CL, respectively, defined with 2 DOF. The left (right) two panels are for $\sin^2 2\theta_{13} = 0.01$ (0.001). The upper two panels are for the systematic errors $\sigma_{PB} = \sigma_{Pb} = \sigma_{pB} = 2\%$ and $\sigma_{pb} = 1\%$ as described in the text, and the lower two panels are with a factor of 2 larger (apply to all) errors. The normal mass hierarchy is assumed and CP phase is taken to be $\delta = 0$.

tive to density change and measurement is still dominated by the statistical error.

Different roles played by various errors which lead to the enhanced uncertainties should be mentioned. The factor 2 larger overall normalization error σ_{PB} primarily affects the uncertainty in $\sin^2 2\theta_{13}$ as expected, and gives little effect to the uncertainty of matter density $\delta\rho$. The increasing error of $\delta\rho/\rho$ is due to accumulation of small and comparable contributions by the other three kind of the systematic errors, σ_{Pb}, σ_{pB}, and σ_{pb}. The enhanced error of $\sin^2 2\theta_{13}$, on the other hand, is contributed mostly by σ_{PB} and σ_{pB} apart from minor contribution from σ_{Pb}.

Here are some comments on the effects of including the energy resolution and possible values of Δm^2_{31} different from the standard one. The numbers presented below are for the case of normal mass hierarchy but we have checked that the situation is similar in the case of inverted hierarchy. The CP phase δ is taken to be $\delta = 0$.

(1) Because we use only two wide ranged energy bins, it is likely that including the energy resolution into our analysis gives only a minor effect to the sensitivity to $\delta\rho/\rho$. To confirm this point explicitly we have included the energy resolution into the analysis by assuming the Gaussian form with width $\sigma_E = 0.15E$ GeV (as taken in [27]). At $\sin^2 2\theta_{13} = 0.01$, $\delta\rho/\rho$ becomes worse from 0.81% (without σ_E) to 0.86% (with σ_E). At $\sin^2 2\theta_{13} = 0.001$, the corresponding numbers are 1.8% (without σ_E) and 1.9% (with σ_E). Since the effect of σ_E is so minor we ignore the energy resolution in our subsequent analysis.

(2) If the value of Δm^2_{31} is larger than $\Delta m^2_{31} = 2.5 \times 10^{-3}$ eV^2 which is assumed in our analysis, there is no problem; $\delta\rho/\rho$ is comparable or smaller than the one obtained above. However, if the value of Δm^2_{31} is smaller, the sensitivity to $\delta\rho/\rho$ becomes less. If we assume $\Delta m^2_{31} = 1.5 \times 10^{-3}$ eV^2, the lower limit allowed by the Super-Kamiokande data (the last reference in [1]), we have to lower the critical energy E_c in defining the energy bins. We have used $E_c = 8$ GeV and $E_c = 10$ GeV for the neutrino and the antineutrino channels, respectively. The obtained sensitivity to $\delta\rho/\rho$ becomes worse but only moderately from the ones quoted above to 1% and 2% at $\sin^2 2\theta_{13} = 0.01$ and 0.001, respectively. We note, however, that the latest value of Δm^2_{31} from the MINOS experiment is higher, $\Delta m^2_{31} = 2.74 \pm^{0.44}_{0.26}$ eV^2 (1σ CL), and that the accuracy of determination must be greatly improved by the T2K and the NOνA experiments.

B. Analysis with varied δ

We now turn to the analysis with varied δ; During the fit we vary δ with addition of $\Delta\chi^2_\delta$ in (11). In Fig. 3, we present the fractional error $\delta\rho/\rho$ as a function of $\sin^2 2\theta_{13}$ at 1, 2, and 3σ CL. Hereafter, the uncertainty $\delta\rho$ is defined with 1 DOF by marginalizing $\sin^2 2\theta_{13}$. The upper and the lower two panels in Fig. 3 are for the normal mass hierarchy with $\delta = 0$ and for the inverted mass hierarchy with $\delta = 4\pi/3$, respectively. As we will fully discuss in Sec. VII the accuracy is the best at around $\delta = 0$ and $\delta = \pi$ in the normal and the inverted hierarchies, respectively. The case of $\delta = 4\pi/3$ is shown in Fig. 3 to indicate that the δ-dependence (which exists only in the small θ_{13} region) is mild and to avoid confining ourselves into the CP conserving values of δ. It should be mentioned here that, though we have varied δ for proper analysis procedure, it does not produce, apart from region of very small θ_{13}, any sizable changes in the results, in accord with the natural expectation.

Notice the remarkable accuracy of determination of the matter density ρ at the magic baseline represented in Fig. 3; The uncertainty is only about 1% at $\sin^2 2\theta_{13} = 0.01$ at 1σ CL for both the normal and the inverted mass hierarchies. At $\sin^2 2\theta_{13} = 0.001$, the uncertainty increases to about 2% (2.5%) at 1σ CL for the case of the normal (inverted) mass hierarchy. At $\sin^2 2\theta_{13} = 0.0001$, however, $\delta\rho/\rho$ becomes worse to about 3% (4%) at 1σ CL for the case of the normal (inverted) mass hierarchy.

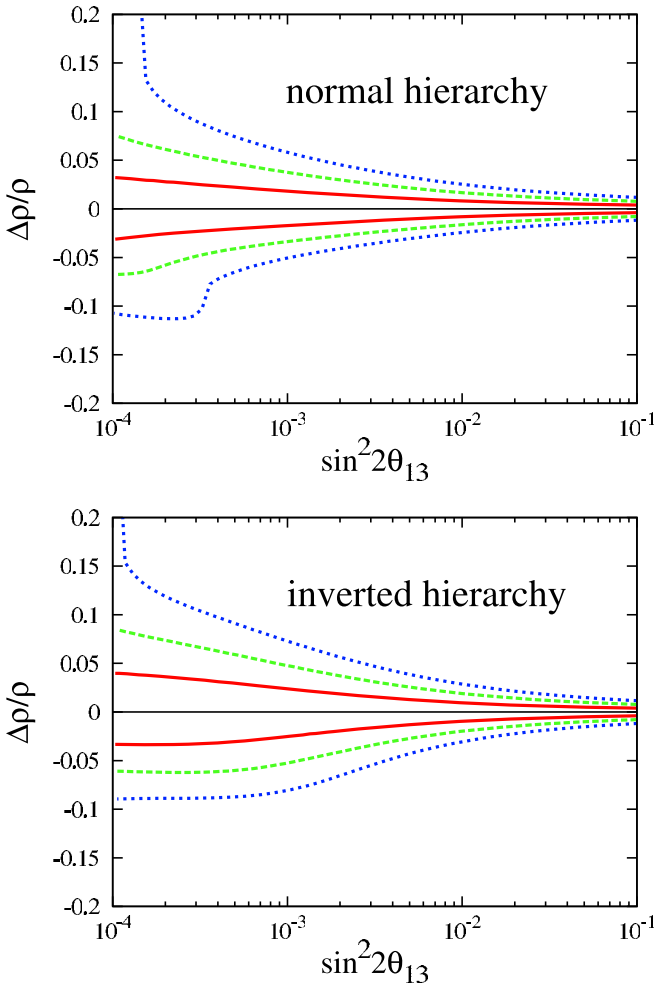

FIG. 3 (color online). The fractional errors in the matter density determination $\delta\rho/\rho$ at 1, 2, and 3σ CL defined with 1 DOF by marginalizing θ_{13} are plotted as a function of $\sin^2 2\theta_{13}$ by the red solid, the green dash-dotted, and the blue dotted lines, respectively. The upper panel is for the normal mass hierarchy with $\delta = 0$ and the lower panel for the inverted mass hierarchy with $\delta = 4\pi/3$.

Unfortunately, however, we have to mention that a subtlety exists on δ-dependence of the sensitivity, which is quite unexpected from the usually advertised nature of the magic baseline. It will be fully discussed in the next section.

Before entering into the problem, let us note the following:

(1) We have explicitly confirmed by plotting $\delta\rho/\rho$ as a function of L that distances comparable to the magic baseline are the right distances for accurate determination of the earth matter density in the energy binning method. In fact, the fractional error $|\delta\rho/\rho|$ has broad minima in the region of distance $L =$ 7000–9000 km if δ is fixed, and $L =$ 7500–9000 km if δ is varied. See Fig. 5.5 in [42]. (The former exercise is to avoid extra complication due to δ dependence which exists in the oscillation probabilities in general except for the magic baseline.)

(2) We have also investigated the possibility that the accuracy of the determination of the earth matter density can be improved by doing an energy scan as well as neutrino energy binning, but without success.

VII. δ DEPENDENCE OF UNCERTAINTY IN MATTER DENSITY DETERMINATION

Despite the remarkable accuracy presented in Fig. 3, it is not the end of our work. We must address the issue of a rather strong δ-dependence in the fractional error $\delta\rho/\rho$ at small θ_{13}, which significantly alters the feature of the results presented above, as the "best cases" with the particular values of δ chosen.

In Fig. 4, presented is the fractional uncertainty $\delta\rho/\rho$ at 1σ CL defined with 1 DOF as a function of δ for four different values of θ_{13}, $\sin^2 2\theta_{13} = 0.1$ (red solid line), $\sin^2 2\theta_{13} = 0.01$ (green dashed line), $\sin^2 2\theta_{13} = 0.003$ (blue short-dashed line), $\sin^2 2\theta_{13} = 0.001$ (magenta dotted line), $\sin^2 2\theta_{13} = 0.0001$ (light-blue dash-dotted line). There is a significant difference between the cases of small and large θ_{13} separated by a critical value, $\sin^2 2\theta_{13} \simeq$ a few $\times 10^{-3}$. At larger θ_{13} than the critical value, the sensitivity to matter density is excellent; The fractional error $\delta\rho/\rho$ is about 0.43%, 1.3%, and $\lesssim 3\%$ at 1σ CL at $\sin^2 2\theta_{13} = 0.1$, 10^{-2}, and 3×10^{-3}, respectively, for all values of δ. It is also notable that δ-dependence of $\delta\rho/\rho$ is very mild in the large θ_{13} region, which confirms the naive expectation due to independence on δ at the magic baseline.

At small θ_{13}, however, there exists a significant δ-dependence in $\delta\rho/\rho$. Despite the fact that the $\delta\rho/\rho$ remains rather small in most of the region of δ, about 4%–6% even at $\sin^2 2\theta_{13} = 10^{-4}$, there are some "spike" structures in $\delta\rho/\rho$ at around $\delta \approx \pi$ for the normal hierarchy and $\delta \approx 0$ for the inverted hierarchy around which $\delta\rho/\rho$ blows up to 15%–20%. They arise when a separated "island" that appear in 1σ CL equi-χ^2 contour merges with the "mainland" 1σ CL allowed region. In our analysis we do not make a sophisticated treatment to take into account separated islands in estimating the errors. Therefore, $\delta\rho/\rho$ in regions near the spike is not quantitatively reliable. On the other hand, the intricate structure of the equi-χ^2 contour suggest that it is unstable to inclusion of additional informations. Namely, a significant improvement of the sensitivity can be expected in the small θ_{13} region by a combined analysis of the intermediate and the far detectors.

Apart from the small structures there seems to be a relationship between the values of δ with a worst sensitivity in the normal and the inverted mass hierarchies as $\delta(\text{worst})_{\text{normal}} \approx \delta(\text{worst})_{\text{inverted}} + \pi$. The strong δ-dependence of the sensitivity including this feature is

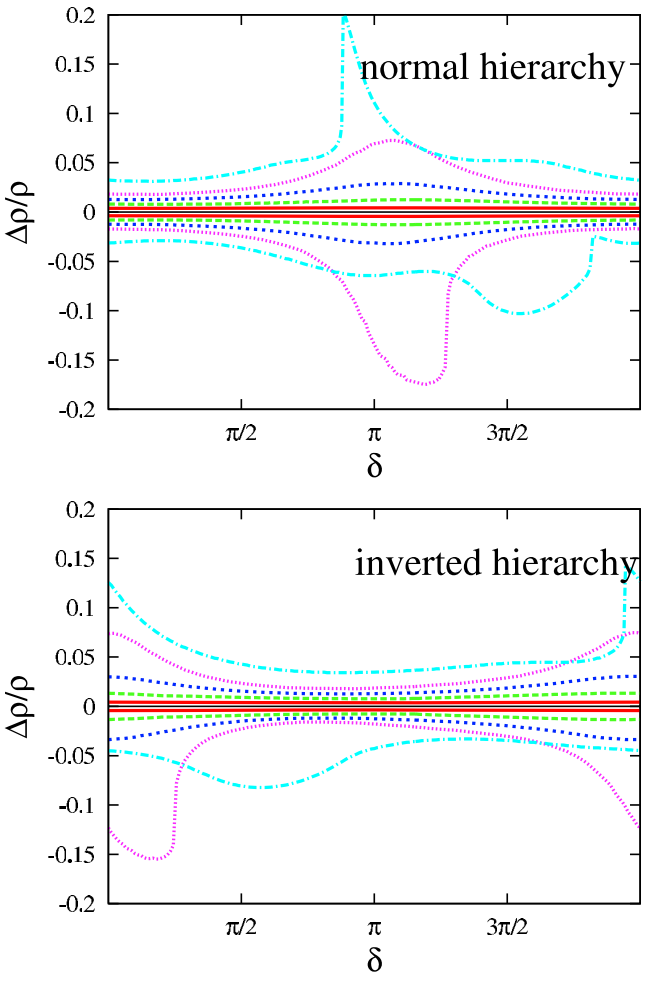

FIG. 4 (color online). Presented are the fractional errors $\delta\rho/\rho$ at 1σ CL with 1 DOF as a function of δ for five different values of θ_{13}, $\sin^2 2\theta_{13} = 0.1$ (red solid line), $\sin^2 2\theta_{13} = 0.01$ (green dashed line), $\sin^2 2\theta_{13} = 0.003$ (blue short-dashed line), $\sin^2 2\theta_{13} = 0.001$ (magenta dotted line), $\sin^2 2\theta_{13} = 0.0001$ (light-blue dash-dotted line). The upper and the lower panels are for the normal and the inverted mass hierarchies, respectively.

quite an unexpected subtlety because we usually think of the magic baseline as the distance where the *CP* phase δ plays minor role. Therefore, the feature should be understood better and it is the reason why we devote the rest of the present section to analyzing the subtlety.

The standard form of oscillation probabilities in $\nu_\mu \to \nu_e$ and $\bar{\nu}_\mu \to \bar{\nu}_e$ channels are given by [15]

$$P(\nu_e \to \nu_\mu) = X_\pm \sin^2 2\theta_{13} + Y_\pm \sin 2\theta_{13} \cos(\delta \mp \Delta_{31}) + P_\odot \tag{12}$$

$$P(\bar{\nu}_e \to \bar{\nu}_\mu) = \bar{X}_\pm \sin^2 2\theta_{13} + \bar{Y}_\pm \sin 2\theta_{13} \cos(\delta \pm \Delta_{31}) + P_\odot = X_\mp \sin^2 2\theta_{13} - Y_\mp \sin 2\theta_{13} \cos(\delta \pm \Delta_{31}) + P_\odot \tag{13}$$

where the functions $X_\pm$ and $Y_\pm$ are defined by

$$X_\pm = s_{23}^2 \left[\frac{\Delta_{31} \sin(aL \mp \Delta_{31})}{(aL \mp \Delta_{31})} \right]^2, \tag{14}$$

$$Y_\pm = \pm 2\sqrt{X_\pm P_\odot} = \pm 2 \sin 2\theta_{12} c_{23} s_{23} \left[\frac{\Delta_{31} \sin(aL \mp \Delta_{31})}{(aL \mp \Delta_{31})} \right] \times \left[\frac{\Delta_{21} \sin(aL)}{aL} \right] \tag{15}$$

$$P_\odot = c_{23}^2 \sin^2 2\theta_{12} \left[\frac{\Delta_{21} \sin(aL)}{aL} \right]^2 \tag{16}$$

where $\pm$ indicates the sign of Δm^2_{31} and $\Delta_{21} \equiv \Delta m^2_{21} L/4E$. In the last line in (13) we have used the relationship [19] between the coefficients $X_\pm$ and $Y_\pm$ in neutrino and antineutrino channels, $\bar{X}_\pm = X_\mp$ and $\bar{Y}_\pm = -Y_\mp$.

We perturb the matter density around the one corresponding to the magic baseline as $aL = \pi + \epsilon$. We expand the neutrino and the antineutrino oscillation probabilities by ϵ and obtain and obtain, to first order in ϵ,

$$P(\nu_e \to \nu_\mu) = P(\nu_e \to \nu_\mu; aL = \pi) - \frac{2\epsilon}{\pi} c_{23} s_{23} \sin 2\theta_{13} \Delta_{21} \Delta_{31} \frac{\sin\Delta_{31}}{(\pi \mp \Delta_{31})} \times \left[\cos(\delta \mp \Delta_{31}) + \frac{\pi \Delta_{31}}{\Delta_{21}(\pi \mp \Delta_{31})} \times \frac{\sin 2\theta_{13} \tan\theta_{23}}{\sin 2\theta_{12}} \left(\frac{\sin\Delta_{31}}{\pi \mp \Delta_{31}} \pm \cos\Delta_{31} \right) \right], \tag{17}$$

$$P(\bar{\nu}_e \to \bar{\nu}_\mu) = P(\bar{\nu}_e \to \bar{\nu}_\mu; aL = \pi) - \frac{2\epsilon}{\pi} c_{23} s_{23} \sin 2\theta_{13} \Delta_{21} \Delta_{31} \frac{\sin\Delta_{31}}{(\pi \pm \Delta_{31})} \times \left[-\cos(\delta \pm \Delta_{31}) + \frac{\pi \Delta_{31}}{\Delta_{21}(\pi \pm \Delta_{31})} \times \frac{\sin 2\theta_{13} \tan\theta_{23}}{\sin 2\theta_{12}} \left(\frac{\sin\Delta_{31}}{\pi \pm \Delta_{31}} \mp \cos\Delta_{31} \right) \right]. \tag{18}$$

Suppose that values of the parameters are such that the quantity in the square bracket in (17) or (18) cancel out. Then, the measurement loses the sensitivity to density change, leading to an enlarged error in $\delta\rho/\rho$. The phenomenon can take place only if the two terms have the same order of magnitudes, which occurs at small θ_{13}, $\sin 2\theta_{13} \approx \Delta_{21}/\Delta_{31} = |\Delta m^2_{21}/\Delta m^2_{31}| \simeq 1/30$, which ex-

plains why the δ-dependent loss of the sensitivity in Fig. 4 occurs only in region of $\sin^2 2\theta_{13}$ comparable to ~ 0.001.

We note that the event statistics is dominated by the neutrino channel in the normal mass hierarchy, and by the antineutrino channel in the inverted one, one can observe in Fig. 1. Let us focus on these dominant channels. Then, we observe a notable regularity: The values of δ which makes the square brackets in (17) (upper sign) and (18) (lower sign) vanish are related by $\cos(\delta_{\nu;\mathrm{normal}} - \Delta_{31}) + \cos(\delta_{\bar{\nu};\mathrm{inverted}} - \Delta_{31}) = 0$, or $\delta_{\nu;\mathrm{normal}} = \delta_{\bar{\nu};\mathrm{inverted}} + \pi$. It explains the salient feature of Fig. 4, the relationship between the δ's corresponding to the worst sensitivities to $\delta\rho/\rho$ in the normal and the inverted mass hierarchies. One can also verify that with $\Delta_{31} \sim 1$ the equations of vanishing the order ϵ terms in (17) and (18) are roughly consistent with $\delta_{\nu;\mathrm{normal}} \approx \pi$ and $\delta_{\nu;\mathrm{inverted}} \approx 0$.

VIII. GLOBAL FIT VS. ITERATIVE METHOD

In this paper, we have restricted ourselves to the simplified analysis in which information from the intermediate detector is modeled by the effective χ^2 as in (11). Clearly one has to engage in the next step a global analysis of all the data set taken by the intermediate and the far detectors which aims at measuring the earth matter density *in situ* as a part of the program of determining all the relevant lepton flavor mixing parameters.

What is the right way to carry it out? A straightforward answer to this question may be to marginalize (minimize χ^2) with respect to the remaining parameters from the one that one want to determine. Since the allowed region in $\sin^2 2\theta_{13} - \rho$ space is already rather compact with use of the data of only a far detector, the method may produce a satisfactory result by just marginalizing the χ^2.

Nonetheless, we describe here an alternative iterative method for determination of earth matter density in neutrino factory. We start from a zeroth-order assumption of the matter density taken from an estimate (with uncertainties) by geophysical models. Then, the iterative procedure includes the following two steps:

(i) We assume a nth order assumption of the matter density with uncertainties and carry out the analysis to obtain nth order values of θ_{13} and δ.

(ii) We use nth order values of θ_{13} and δ with uncertainties to obtain $(n+1)$th order value of the matter density.

Assuming convergence we expect that the method is able to produce an improved estimate of the three relevant parameters, θ_{13}, δ, and the matter density ρ in a self-consistent way.

We note that, irrespective of which analysis method is employed, one can expect improvement of the accuracies in determination of the matter density. Measurement of the intermediate detector should improve $\delta\rho/\rho$ directly because of its sensitivity to the earth matter effect, in a similar manner as CP phase measurement by the two-detector method [52].[6] We have already mentioned in the previous section the reasons why a significant improvement can be expected at small θ_{13} by combined analysis where a intricate structure of χ^2 minima entails worsened errors in a limited region of δ.

IX. CONCLUDING REMARKS

In this paper, we have demonstrated that an *in situ* precision determination of the earth matter density can be carried out by neutrino factory with a detector placed at the magic baseline. There are two regions which are separated by a critical value of θ_{13}, $\sin^2 2\theta_{13} \simeq$ a few $\times 10^{-3}$. In the large θ_{13} region, the uncertainty $\delta\rho/\rho$ has only mild δ-dependence as expected by the desirable feature of measurement at the magic baseline. The achievable accuracy of matter density determination is excellent; The fractional error $\delta\rho/\rho$ is about 0.43%, 1.3%, and $\lesssim 3\%$ at 1σ CL at $\sin^2 2\theta_{13} = 0.1$, 10^{-2}, and 3×10^{-3}, respectively. It is worthwhile to note that the sensitivity is insensitive against increasing the systematic errors by a factor of 2. These are the good enough accuracies to solve the problem of the notorious uncertainty in the neutrino factory data analysis for precision determination of θ_{13} and the CP phase δ in view of Fig. 24 of [27], for example.

In the smaller θ_{13} region, however, we uncovered a subtle δ-dependence in the accuracy of determination at small θ_{13}. In a certain range of δ it occurs that the responses of the dominant atmospheric term and the solar-atmospheric interference term to matter density variation cancel with each other, leading to reduced sensitivity (spike structure in Fig. 4) in $\delta\rho/\rho$. Adding the ν_μ disappearance channel does not appear to help. We were unable to solve this problem within the framework of analysis used in this paper. We, however, emphasize that $\delta\rho/\rho$ remains small in most of the region of δ; At $\sin^2 2\theta_{13} = 10^{-4}$ it is 3%–7% at 1σ CL in more than 3/4 of the entire region of δ. Furthermore, we expect that simultaneous analysis of the intermediate and the far detector data should improve the situation significantly, as discussed in Sec. VII. If it works it resolves the long debated problem of obscured CP violation by the uncertainty of the earth matter density.

It should be stressed, among other things, is that this apparatus seems to provide the most accurate way to directly measure the matter density inside the earth. It will provide a stringent test for geophysical estimation of the matter density and/or the MSW theory of neutrino propagation in matter.

[6] See Fig. 2 in [53] obtained in the analysis for the first reference in [39] for demonstration of this point.

Finally, we want to mention about other possible ways which could provide with us different ways of measuring matter density or alternative means of testing the MSW theory.

(i) The transition region of ^{8}B neutrinos from the sun in the energy region of 3–4 MeV, if measured with precision, would allow us to accurately determine the matter density in the solar interior. Given the fact that we have two alternative ways to cross check the results, helioseismology and the standard solar model calculation, this possibility may give another good way for a stringent test of the MSW theory of neutrino propagation in matter.

(ii) As one can learn from the expression of the oscillation probability (12) and (13) the relative importance of the matter effect to the vacuum effect in neutrino oscillation is not controlled completely by the ratio aL/Δ_{31}. It may open the possibility of using other variables as tunable parameters, e.g., the baseline L. It would then be interesting to examine this possibility in the light of recent proposal of the Tokai-to-Kamioka-Korea (T2KK) project [39,54]. Because of the identical two-detector setting, it would allow us to accurately determine the matter density in the crust region below the sea of Japan.

(iii) Finally, we want to note that measuring the matter density and confronting it to another method is *not* the only way to verify the MSW theory. For example, the concept of mass eigenstate in matter as well as the regeneration of neutrino flavors are best tested by observing the day-night effect in solar neutrino observation.

ACKNOWLEDGMENTS

We thank the Theoretical Physics Department of Fermilab for hospitality extended to us during the visit in the summer 2005 when this work was initiated. One of the authors (H. M.) is grateful to Maria Gonzalez-Garcia for useful discussions in an infant stage of this work. He thanks Alexei Smirnov for his illuminating comments and to Abdus Salam International Center for Theoretical Physics for hospitality. The other (S. U.) thanks Olga Mena for discussions about details of the analysis in [15]. This work was supported in part by the Grant-in-Aid for Scientific Research, No. 16340078, Japan Society for the Promotion of Science.

[1] Y. Fukuda *et al.* (Kamiokande Collaboration), Phys. Lett. B **335**, 237 (1994); Y. Fukuda *et al.* (Super-Kamiokande Collaboration), Phys. Rev. Lett. **81**, 1562 (1998); Y. Ashie *et al.* (Super-Kamiokande Collaboration), Phys. Rev. D **71**, 112005 (2005).

[2] B. T. Cleveland *et al.*, Astrophys. J. **496**, 505 (1998); J. N. Abdurashitov *et al.* (SAGE Collaboration), Phys. Rev. C **60**, 055801 (1999); W. Hampel *et al.* (GALLEX Collaboration), Phys. Lett. B **447**, 127 (1999); M. Altmann *et al.* (GNO Collaboration), Phys. Lett. B **616**, 174 (2005); J. Hosaka *et al.* (Super-Kamiokande Collaboration), Phys. Rev. D **73**, 112001 (2006); Q. R. Ahmad *et al.* (SNO Collaboration), Phys. Rev. Lett. **87**, 071301 (2001); **89**, 011301 (2002); B. Aharmim *et al.* (SNO Collaboration), Phys. Rev. C **72**, 055502 (2005).

[3] K. Eguchi *et al.* (KamLAND Collaboration), Phys. Rev. Lett. **90**, 021802 (2003).

[4] Y. Ashie *et al.* (Super-Kamiokande Collaboration), Phys. Rev. Lett. **93**, 101801 (2004).

[5] T. Araki *et al.* (KamLAND Collaboration), Phys. Rev. Lett. **94**, 081801 (2005).

[6] E. Aliu *et al.* (K2K Collaboration), Phys. Rev. Lett. **94**, 081802 (2005).

[7] D. G. Michael *et al.* (MINOS Collaboration), Phys. Rev. Lett. **97**, 191801 (2006).

[8] Z. Maki, M. Nakagawa, and S. Sakata, Prog. Theor. Phys. **28**, 870 (1962).

[9] The idea of conventional superbeam for measuring *CP* violation may be traced back to: H. Minakata and H. Nunokawa, Phys. Lett. B **495**, 369 (2000); J. Sato, Nucl. Instrum. Methods Phys. Res., Sect. A **472**, 434 (2001); B. Richter, hep-ph/0008222.

[10] S. Geer, Phys. Rev. D **57**, 6989 (1998); **59**, 039903(E) (1999); A. De Rujula, M. B. Gavela, and P. Hernandez, Nucl. Phys. **B547**, 21 (1999).

[11] P. Zucchelli, Phys. Lett. B **532**, 166 (2002).

[12] M. Apollonio *et al.*, hep-ph/0210192; C. Albright *et al.*, hep-ex/0008064.

[13] J. Bouchez, M. Lindroos, and M. Mezzetto, in *Neutrino Factories and Superbeams*, edited by A. Para, AIP Conf. Proc. No. 721 (AIP, New York, 2004), 37.

[14] A. Baldini *et al.* (BENE Steering Group), "*Beams for European Neutrino Experiments (BENE): Midterm Scientific Report*" (unpublished); C. Albright *et al.* (Neutrino Factory/Muon Collider Collaboration), physics/0411123.

[15] A. Cervera, A. Donini, M. B. Gavela, J. J. Gomez Cadenas, P. Hernandez, O. Mena, and S. Rigolin, Nucl. Phys. **B579**, 17 (2000); **B593**, 731(E) (2001).

[16] L. Wolfenstein, Phys. Rev. D **17**, 2369 (1978).

[17] S. P. Mikheyev and A. Yu. Smirnov, Yad. Fiz. **42**, 1441 (1985) [Sov. J. Nucl. Phys. **42**, 913 (1985)]; Nuovo Cimento Soc. Ital. Fis. C **9**, 17 (1986).

[18] J. Arafune, M. Koike, and J. Sato, Phys. Rev. D **56**, 3093 (1997); **60**, 119905(E) (1997).

[19] H. Minakata and H. Nunokawa, Phys. Rev. D **57**, 4403 (1998).

[20] M. Freund, M. Lindner, S. T. Petcov, and A. Romanino,

Nucl. Phys. **B578**, 27 (2000).
[21] H. Minakata and H. Nunokawa, J. High Energy Phys. 10 (2001) 001.
[22] M. Koike, T. Ota, and J. Sato, Phys. Rev. D **65**, 053015 (2002).
[23] J. Burguet-Castell, M. B. Gavela, J. J. Gomez-Cadenas, P. Hernandez, and O. Mena, Nucl. Phys. **B608**, 301 (2001).
[24] J. Pinney and O. Yasuda, Phys. Rev. D **64**, 093008 (2001).
[25] P. Huber, M. Lindner, and W. Winter, Nucl. Phys. **B645**, 3 (2002).
[26] T. Ohlsson and W. Winter, Phys. Rev. D **68**, 073007 (2003).
[27] P. Huber, M. Lindner, M. Rolinec, and W. Winter, Phys. Rev. D **74**, 073003 (2006).
[28] R. J. Geller and T. Hara, Nucl. Instrum. Methods Phys. Res., Sect. A **503**, 187 (2003).
[29] A. Cervera, Eighth International Workshop on the Neutrino Factories, Superbeams, and Beta Beams, University of California, Irvine, USA, 2006.
[30] For Reference Earth Model, see e.g., the website; http://cfauvcs5.harvard.edu/lana/rem/index.htm.
[31] G. Fogli and E. Lisi, New J. Phys. **6**, 139 (2004).
[32] W. Winter, Phys. Lett. B **613**, 67 (2005).
[33] W. Winter, Phys. Rev. D **72**, 037302 (2005).
[34] M. Lindner, T. Ohlsson, R. Tomas, and W. Winter, Astropart. Phys. **19**, 755 (2003).
[35] For an extensive bibliography, see W. Winter, physics/0602049.
[36] J. E. Campagne, M. Maltoni, M. Mezzetto, and T. Schwetz, hep-ph/0603172.
[37] Y. Itow *et al.*, hep-ex/0106019. For an updated version, see: http://neutrino.kek.jp/jhfnu/loi/loi.v2.030528.pdf.
[38] H. Minakata and H. Nunokawa, Nucl. Instrum. Methods Phys. Res., Sect. A **503**, 218 (2003).
[39] M. Ishitsuka, T. Kajita, H. Minakata, and H. Nunokawa, Phys. Rev. D **72**, 033003 (2005); T. Kajita, H. Minakata, S. Nakayama, and H. Nunokawa, Phys. Rev. D **75**, 013006 (2007).
[40] P. Huber and W. Winter, Phys. Rev. D **68**, 037301 (2003).
[41] A. Y. Smirnov, hep-ph/0610198. For earlier discussions, see e.g., Phys. Scr. T **t121**, 57 (2005).
[42] S. Uchinami, Master of Science Thesis, Tokyo Metropolitan University, 2007 (in Japanese), http://musashi.phys.metro-u.ac.jp/thesis.html.
[43] V. Barger, D. Marfatia, and K. Whisnant, Phys. Rev. D **65**, 073023 (2002).
[44] K. Kimura, A. Takamura, and H. Yokomakura, Phys. Lett. B **537**, 86 (2002).
[45] R. Gandhi, P. Ghoshal, S. Goswami, P. Mehta, and S. Uma Sankar, Phys. Rev. Lett. **94**, 051801 (2005); Phys. Rev. D **73**, 053001 (2006).
[46] A. Blondel, A. Cervera-Villanueva, A. Donini, P. Huber, M. Mezzetto, and P. Strolin, Acta Phys. Pol. B **37**, 2077 (2006).
[47] K. Long, Eighth International Workshop on the Neutrino Factories, Superbeams, and Beta Beams, University of California, Irvine, USA, 2006.
[48] M. Ellis, Eighth International Workshop on the Neutrino Factories, Superbeams, and Beta Beams, University of California, Irvine, USA, 2006.
[49] H. Minakata and H. Sugiyama, Phys. Lett. B **580**, 216 (2004).
[50] R. Raja and A. Tollestrup, Phys. Rev. D **58**, 013005 (1998).
[51] P. Huber, M. Lindner, and W. Winter, J. High Energy Phys. 05 (2005) 020.
[52] H. Minakata and H. Nunokawa, Phys. Lett. B **413**, 369 (1997).
[53] H. Minakata, Phys. Scr. **t127**, 73 (2006).
[54] For broader aspects of "T2KK" visit the web pp.: http://t2kk.snu.ac.kr/ (2nd International Workshop on a Far Detector in Korea for the J-PARC Neutrino Beam, 2006); http://newton.kias.re.kr/hepph/J2K/ (1st International Workshop, 2005).